

The derivation of structure information from the measurements was restricted by experimental resolutions and sensitivities and by the isotopic complexity of the natural elements employed in the work. Despite these restrictions the experiments indicated that there were omissions and/or inappropriate spin and parity assignments in the reported low-energy excited structure of both Ta and Re. Revisions of the excited structure of Ta consistent with the unified model and experimental observation were proposed. Modifications of and ad-

ditions to the reported structure of Re were suggested by the experimental results inclusive of a specific state attributed to a predicted single-particle configuration in Re¹⁸⁵.

ACKNOWLEDGMENTS

The authors are appreciative of assistance rendered by a number of members of the Applied Nuclear Physics Section, Reactor Physics Division, Argonne National Laboratory.

^{90,92,94}Zr(*p, p'*) Reactions at 12.7 MeV*

J. K. DICKENS, E. EICHLER, AND G. R. SATCHLER
Oak Ridge National Laboratory, Oak Ridge, Tennessee
(Received 22 November 1967)

The elastic and inelastic scattering of 12.7-MeV protons from ^{90,92,94}Zr has been studied. Angular distributions for the elastic and 40 inelastic groups were measured. An optical-model analysis of the elastic scattering was performed. The inelastic scattering was interpreted, using the usual "collective"-model interaction and the distorted-wave approximation. Multipolarities *L* were assigned where possible, and strength parameters β_L were deduced. The inelastic scattering to some states was also compared with the predictions of the shell model, using a simple two-body interaction of Yukawa type and including the effects of core polarization. Reasonable agreement was obtained, although the angular distributions for the 0⁺ and 3⁻ excitations imply that a more sophisticated effective interaction is required.

I. INTRODUCTION

THE excitation of levels in ⁹⁰Zr by 18.8-MeV protons¹ and in ^{92,94}Zr by 19.4-MeV protons² has been reported recently and the measurements were interpreted in terms of a microscopic description of the interaction, using shell-model wave functions for the target nuclei.^{3,4} The apparent success of this analysis lent additional interest to obtaining similar data at other energies. Partly for this reason, measurements on these nuclei were also made using 12.7-MeV protons. In addition, better energy resolution was obtained than at the higher energies and a few new transitions were detected. In particular, angular distributions were obtained for the excitation of the lowest 0⁺ excited state in each isotope, and these are of considerable theoretical interest.

Inelastic scattering from these isotopes provides a useful testing ground for the microscopic description of

the interaction because often the states of low excitation may be identified with simple shell-model configurations involving very few valence nucleons.⁵ The model takes a two-body "effective" interaction between the projectile and each target nucleon. The earlier analyses³ were directed toward determining the parameters of this effective interaction. Since then it has been realized that, in addition to the direct interaction between the projectile and the valence nucleons of the target, there are important contributions due to virtual excitations of the core nucleons.⁶ (The same contributions give rise to the need to use effective charges for the valence nucleons in electromagnetic transitions.) The parameters for these core polarization terms are often not known. Hence there is a corresponding uncertainty in deducing the parameters of the direct coupling between projectile and valence nucleon. For this reason, less was learned from the data to be reported here than had been hoped originally. Nonetheless, the data are an important check for any further developments of the theory.

Since this work was completed, measurements of the scattering of 14.5-MeV protons by ^{90,92}Zr have been reported.⁷ The measurements are not as extensive as

* Research sponsored by the U. S. Atomic Energy Commission under contract with Union Carbide Corporation.

¹ W. S. Gray, R. A. Kenefick, J. J. Kraushaar, and G. R. Satchler, Phys. Rev. **142**, 735 (1966).

² M. M. Strautberg and J. J. Kraushaar, Phys. Rev. **151**, 969 (1966).

³ M. B. Johnson, L. W. Owen, and G. R. Satchler, Phys. Rev. **142**, 748 (1966); G. R. Satchler, Nucl. Phys. **A95**, 1 (1967).

⁴ H. O. Funsten, N. R. Roberson, and E. Rost, Phys. Rev. **134**, B117 (1964); V. A. Madsen and W. Tobocman, *ibid.* **139**, B864 (1965); N. K. Glendenning and M. Veneroni, *ibid.* **144**, 739 (1966); G. R. Satchler, Nucl. Phys. **77**, 481 (1966); V. A. Madsen, *ibid.* **80**, 177 (1966).

⁵ B. F. Bayman, A. S. Reiner, and R. K. Sheline, Phys. Rev. **115**, 1627 (1959); I. Talmi and I. Unna, Nucl. Phys. **19**, 225 (1960); I. Talmi, Phys. Rev. **126**, 2116 (1962).

⁶ W. G. Love and G. R. Satchler, Nucl. Phys. **A92**, 11 (1967).

⁷ K. Matsuda, H. Nakamura, I. Nonaka, H. Taketani, T. Wada, Y. Awaya, and M. Koike, J. Phys. Soc. Japan **22**, 1311 (1967).

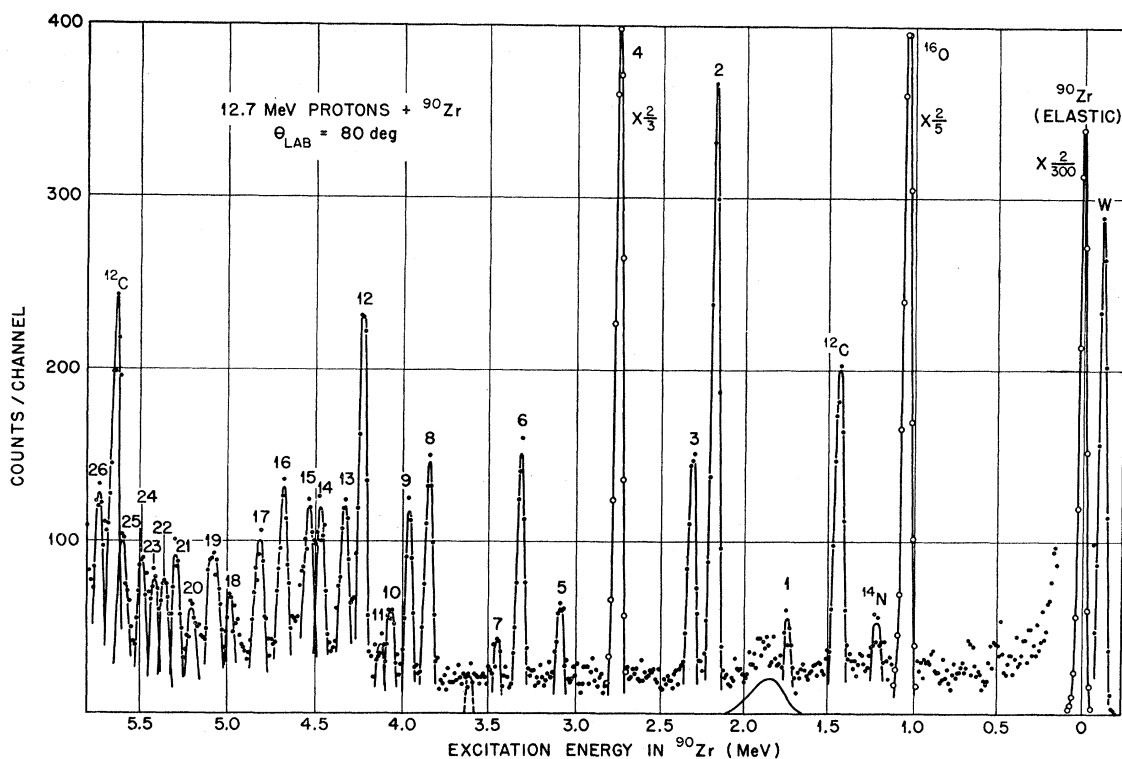


FIG. 1. Pulse-height spectrum of protons scattered from ^{90}Zr . Proton groups associated with scattering from contaminant nuclei are labelled with the symbol for that nucleus. The numbered groups correspond to proton excitation of levels in ^{90}Zr as listed in Table I.

TABLE I. Excited states of ^{90}Zr . The peak number corresponds to the numbering in Fig. 1. The errors for the excitation energies E_x are less than 1%. The L values correspond to the curves shown in the figures and the β_L values are those used to normalize those curves. Spin-parity assignments in parentheses are tentative.

Peak No.	E_x (MeV)	J^π	L	β_L
1	1.75	0^+	0	
2	2.18	2^+	2	0.075
3	2.32	5^-	5	0.09
4	2.74	3^-	3	0.17
5	3.09	4^+	4	0.053
6	3.31	2^+	2	0.06
7	3.45	6^+	6	0.04
8	3.85	2^+	2	0.06
9	3.97	5^-	5	0.09
10	4.07	(3^-)	$\begin{cases} 3 \\ 5 \end{cases}$	$\begin{cases} 0.05 \\ 0.066 \end{cases}$
11	4.12		$\begin{cases} 2 \\ 2 \end{cases}$	$\begin{cases} 0.03 \\ 0.09 \end{cases}$
12	4.23		$\begin{cases} 2 \\ 5 \end{cases}$	$\begin{cases} 0.09 \\ 0.13 \end{cases}$
13	4.33	4^+	4	0.08
14	4.47		$\begin{cases} 2 \\ 4 \end{cases}$	$\begin{cases} 0.07 \\ 0.07 \end{cases}$
15	4.54		2	0.07
16	4.68	(2^+)	2	0.07
17	4.82			
18	4.99	(2^+)	2	0.045
19 ^a	5.08		$\begin{cases} 3 \\ 4 \end{cases}$	$\begin{cases} 0.07 \\ 0.08 \end{cases}$
20	5.20			
21	5.29			
22	5.36			
23	5.42			
24	5.49			
25	5.60 ^b			
26	5.73			

^a This proton group is wider than expected for a single level.

^b Peak position determined at other angles where ^{12}C contaminant does not interfere.

the present data, and the analysis is limited to comparison of the inelastic data with collective-model predictions. The conclusions obtained from the 14.5-MeV work are substantially in agreement with the present conclusions.

II. EXPERIMENTAL DETAILS

The 12.7-MeV proton beam from the ORNL Tandem Van de Graaff Accelerator impinged on targets of ^{90}Zr , ^{92}Zr , and ^{94}Zr (with isotopic enrichments of 98, 93, and 97%, respectively), each target having a thickness of about 1 mg/cm². The scattered protons were observed with a solid-state surface-barrier detector having a depletion layer deep enough to fully stop 13-MeV protons with approximately 40-keV full width at half maximum (FWHM) resolution. The beam intensity was monitored by a standard Faraday cup and by a second solid-state detector placed at 90° to the beam. Pulse-height spectra were obtained for each target at 5° intervals for laboratory angles between 25° and 165°.

The spectrum shown in Fig. 1 was taken at $\theta_{\text{lab}}=80^\circ$ for protons scattered from ^{90}Zr , and shows proton groups for excitations in ^{90}Zr up to about 5.5 MeV. Excitation energies for the levels of ^{90}Zr obtained from these data are given in Table I. The broad group shown in Fig. 1 at $E_x \sim 1.8$ MeV is the detector escape peak.⁸ Our resolution was adequate to resolve the proton group

⁸ J. K. Dickens, F. G. Perey, and R. J. Silva, Phys. Rev. **132**, 1190 (1963).

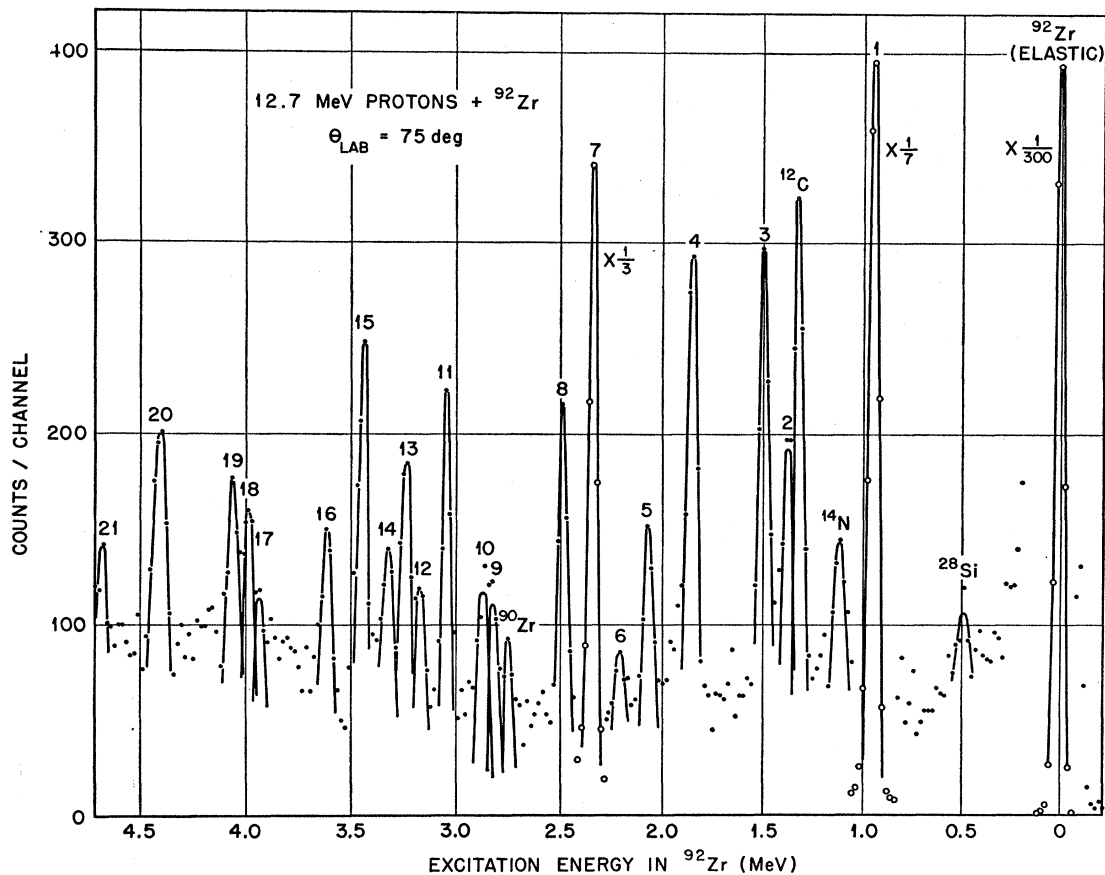


FIG. 2. Pulse-height spectrum of protons scattered from ^{92}Zr . Proton groups associated with shattering from contaminant nuclei are labeled with the symbol for that nucleus. The numbered groups correspond to proton excitation of levels in ^{92}Zr as listed in Table II.

due to scattering from the first excited 0^+ level in ^{90}Zr with $E_x = 1.75$ MeV, but with increased uncertainties in the differential cross sections extracted for this transition. The dashed peak at $E_x \sim 3.6$ MeV indicates the position expected for a proton group inelastically scattered from the 8^+ level in ^{90}Zr . The cross section for proton excitation of this level is very small at our bombarding energy, apparently because of the centrifugal barrier. A similar effect was observed⁹ in 12-MeV proton scattering from ^{92}Mo . On this basis, we suggest that none of the levels excited in this experiment will have $J > 7$.

The spectrum shown in Fig. 2 was taken at $\theta_{\text{lab}} = 75^\circ$ for protons scattered from ^{92}Zr , and shows proton groups for excitations in ^{92}Zr up to 4.75 MeV. Excitation energies for levels in ^{92}Zr obtained from these data are given in Table II. The proton group at $E_x \sim 2.75$ MeV is due to excitation of the 3^- level of ^{90}Zr (there was about 3% of ^{90}Zr in the ^{92}Zr target); the magnitude and angular distribution for this group is consistent with this assignment. The proton group at $E_x \sim 2.18$ MeV might be thought, similarly, to be due to excitation of the corresponding 2^+ level of ^{90}Zr . However, the

TABLE II. Excited states of ^{92}Zr . The peak number corresponds to the numbering in Fig. 2. The errors for the excitation energies E_x are less than 1% except for the values in parentheses. The L values correspond to the curves shown in the figures and the β_L values are those used to normalize those curves. Spin-parity assignments in parentheses are tentative.

Peak No.	E_x (MeV)	J^π	L	β_L
1	0.93	2^+	2	0.13
2	1.37	0^+	0	
3	1.50	4^+	4	0.07
4	1.85	2^+	2	0.055
5	2.07		$\begin{cases} 2 \\ 4 \end{cases}$	$\begin{cases} 0.05 \\ 0.06 \end{cases}$
6	2.18			
7	2.34			
8	2.49	(5^-)	5	0.075
9	(2.83)			
10	(2.86)			
11	3.05		$\begin{cases} 2 \\ 5 \end{cases}$	$\begin{cases} 0.04 \\ 0.07 \end{cases}$
12	3.18			
13	3.24		4	0.06
14	3.32			
15 ^a	3.43		4	0.09
16	3.62			
17	(3.94)			
18	3.99			
19	4.07			
20 ^a	4.41			
21	4.72			

⁹ J. K. Dickens, E. Eichler, R. J. Silva, and G. Chilosi, Phys. Letters 21, 657 (1966).

^a This proton group is wider than expected for a single level.

magnitude of the integrated partial cross section is about twice that expected if only the 2^+ level of ^{90}Zr contributes. Thus, part of this proton group must be due to excitation of a level with $E_x \sim 2.18$ MeV in ^{92}Zr .

The spectrum shown in Fig. 3 was taken at $\theta_{\text{lab}} = 50^\circ$ for protons scattered from ^{94}Zr and shows proton groups for excitations in ^{94}Zr up to 4.5 MeV. Excitation energies for levels in ^{94}Zr obtained from these data are given in Table III. A careful study for impurity contributions was made. In our estimation, all numbered proton groups result from excitation of the nucleus ^{94}Zr .

Energy calibration of the pulse-height system depended upon the positions of the proton peaks due to elastic scattering from the Zr target and to elastic and inelastic scattering in the ^{12}C and ^{16}O target contaminants; corrections for electronic nonlinearity were obtained using a precision pulser. Because of uncertainties inherent in this calibration, we assign an error of ± 30 keV for excitation energies $E_x \sim 4$ MeV, with the error decreasing with decreasing excitation.

For all three targets there were proton peaks with widths greater than our resolution, suggesting proton scattering by more than one level of the target nucleus. An example is the broad peak at $E_x \sim 2.9$ MeV in Fig. 3. This peak was studied carefully in eight pulse-height spectra for laboratory angles between 40° and 80° , using peak-fitting methods. We obtained a good fit to this peak with three peaks (Nos. 10–12 in ^{94}Zr), but we cannot exclude the possibility of additional levels in this group. Other broad groups were similarly analyzed; the resulting less-certain excitation energies are given in parentheses in Tables I–III.

Center-of-mass differential cross sections and associated uncertainties were obtained for elastic scattering from all three targets, and for inelastic scattering from well-separated excited states of each target nucleus. The over-all absolute normalization depends upon accuracy in beam integration, target thickness measurement, and solid-angle determination, and was estimated to be accurate to within 10%. The detector could be

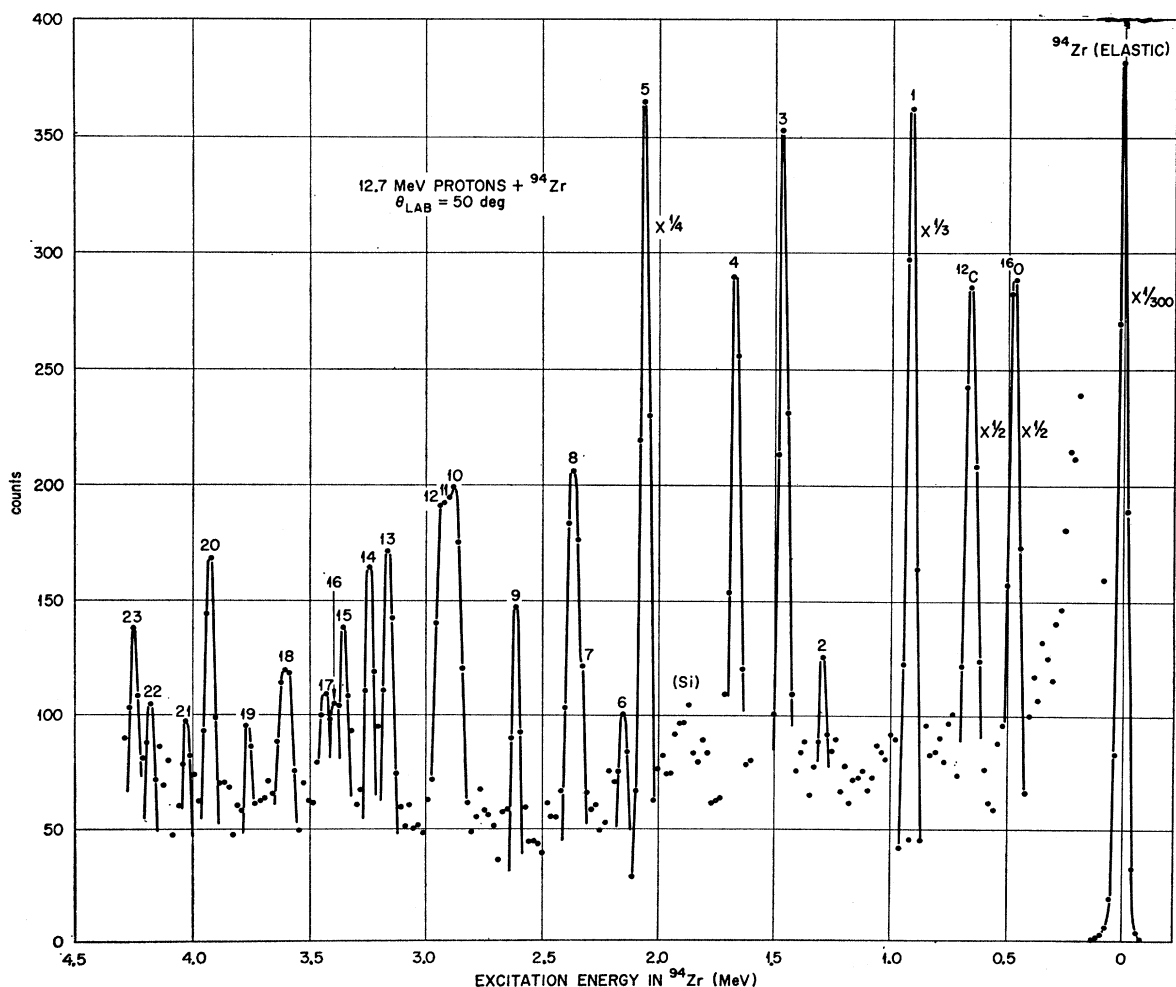


FIG. 3. Pulse-height spectrum of protons scattered from ^{94}Zr . Proton groups associated with scattering from contaminant nuclei are labelled with the symbol for that nucleus. The numbered groups correspond to proton excitation of levels in ^{94}Zr as listed in Table III.

positioned to 0.05° with respect to the geometrical zero line of the scattering chamber; this zero line was determined to be the path of the bombarding proton beam with a precision of 0.2° . The absolute value of the bombarding energy was determined to be 12.7 ± 0.1 MeV; the relative energy did not vary by more than 10 keV throughout the experiment. There were essentially no random errors associated with the elastic scattering measurements. For the inelastic scattering, the largest uncertainty in nearly every differential cross section arose from the estimation of the "background"—due mainly to the "tail" from the elastically scattered protons. Thus, the differential cross sections for the weakly excited states have larger uncertainties than would be assigned if based solely on counting statistical uncertainties. These differential cross sections are available in tabular form in a report¹⁰ which also gives some additional experimental details.

III. OPTICAL-MODEL ANALYSIS OF ELASTIC SCATTERING

The elastic scattering was analyzed in terms of an optical-model potential of the usual form:

$$U(r) = -V(e^x + 1)^{-1} - 4iW_D(d/dx')(e^{x'} + 1)^{-1} + (\hbar/m_\pi c)^2 V_s r^{-1}(d/dr)(e^{x_s} + 1)^{-1} \sigma \cdot \mathbf{l}, \quad (1)$$

where

$x = (r - r_0 A^{1/3})/a$, $x' = (r - r_0' A^{1/3})/a'$, $x_s = (r - r_s A^{1/3})/a_s$, to which is added the Coulomb potential for a uniformly charged sphere of radius $1.25 A^{1/3}$ F. The spin-orbit strength V_s was taken to be real.

The parameter values for which the theoretical calculations best fit the experimental data were determined by use of an automatic search routine¹¹ which minimizes the quantity

$$\chi^2 = N^{-1} \sum_{i=1} \{ [\sigma_{\text{th}}(\theta_i) - \sigma_{\text{exp}}(\theta_i)] / \Delta\sigma_{\text{exp}}(\theta_i) \}^2, \quad (2)$$

where $\sigma_{\text{exp}}(\theta_i)$, $\sigma_{\text{th}}(\theta_i)$ are the measured and calculated differential cross sections, respectively, at angle θ_i , and $\Delta\sigma_{\text{exp}}$ is the weight assigned to σ_{exp} . For convenience, χ^2 was calculated with $\Delta\sigma_{\text{exp}}/\sigma_{\text{exp}} = 5\%$ for all angles.

An analysis of proton scattering for $9 \leq E_p \leq 22$ MeV from many nuclei has been reported by Perey¹² and an average set of "geometrical" parameters was suggested. There were $r_0 = r_0' = r_s = 1.25$ F, $a = a_s = 0.65$ F, and $a' = 0.47$ F. Later work, including studies of polarization data,¹³ suggested independent spin-orbit parameters of $r_s = 1.12$ F and $a_s = 0.47$ F. The initial study of the present data was made with these parameters by searching only on values of V and W_D , keeping $V_s = 6$ MeV fixed.¹³ The results are shown as set *A* in Table IV

¹⁰ J. K. Dickens, E. Eichler, R. J. Silva, and G. Chilosi, Oak Ridge National Laboratory Report No. ORNL-3934, 1966 (unpublished).

¹¹ R. M. Drisko (unpublished).

¹² F. G. Perey, Phys. Rev. **131**, 745 (1963).

¹³ F. G. Perey in *Proceedings of the International Conference on*

TABLE III. Excited states of ^{94}Zr . The peak number corresponds to the numbering in Fig. 3. The errors for the excitation energies E_x are less than 1% except for the values in parentheses. The L values correspond to the curves shown in the figures and the β_L values are those used to normalize those curves. Spin-parity assignments in parentheses are tentative.

Peak No.	E_x (MeV)	J^π	L	β_L
1	0.92	2^+	2	0.13
2	1.30	0^+	0	
3	1.47	4^+	4	0.065
4	1.66	2^+	2	0.065
5	2.06	3^-	3	0.18
6	2.16			
7	(2.32)		2	0.03
8	2.36		$\left\{ \begin{array}{l} 2 \\ 4 \end{array} \right.$	$\left\{ \begin{array}{l} 0.05 \\ 0.06 \end{array} \right.$
9	2.61	(5^-)	5	0.075
10	(2.85)			
11	(2.89)			
12	(2.94)			
13	3.16	4^+	4	0.05
14	3.24		$\left\{ \begin{array}{l} 5 \\ 6 \end{array} \right.$	$\left\{ \begin{array}{l} 0.07 \\ 0.075 \end{array} \right.$
15	3.35			
16	3.39			
17	3.46			
18 ^a	3.60			
19	3.76			
20	3.92		$\left\{ \begin{array}{l} 3 \\ 6 \end{array} \right.$	$\left\{ \begin{array}{l} 0.06 \\ 0.07 \end{array} \right.$
21	4.02			
22	4.18			
23	4.25			

^a This proton group is wider than expected for a single level.

TABLE IV. Optical-model parameters for 12.7-MeV scattering from $^{90,92,94}\text{Zr}$. The values in italics were kept fixed during the search. Constrained spin-orbit coupling with $r_s = r_0$ and $a_s = a$ was used except for sets *A*, *A'*, *B*, and *B'*, where $r_s = 1.12$ F and $a_s = 0.47$ F were used. The primed parameter sets for $^{90,92}\text{Zr}$ were obtained by searching on the cross sections multiplied by 0.90. The χ^2 were computed assuming $\Delta\sigma/\sigma = 5\%$ at all angles, with the number of data $N = 32$ (90), 31 (92), and 30 (94).

Set	<i>A</i>	<i>V</i> (MeV)	<i>r</i> ₀ (F)	<i>a</i> (F)	<i>W</i> _{<i>D</i>} (MeV)	<i>r</i> ' ₀ (F)	<i>a</i> ' (F)	<i>V</i> _{<i>s</i>} (MeV)	σ_A (mb)	χ^2
<i>A</i>	90	51.6	1.25	0.65	13.4	1.25	0.47	6.0	912	4.2
<i>A</i>	92	52.2	1.25	0.65	12.4	1.25	0.47	6.0	915	6.5
<i>A</i>	94	52.2	1.25	0.65	13.0	1.25	0.47	6.0	932	18.2
<i>A'</i>	90	52.0	1.25	0.65	12.8	1.25	0.47	6.0	908	2.6
<i>A'</i>	92	52.1	1.25	0.65	13.4	1.25	0.47	6.0	923	4.5
<i>B</i>	90	52.8	1.25	0.65	15.6	1.25	0.412	6.0	878	2.3
<i>B</i>	92	52.2	1.25	0.65	12.3	1.25	0.525	6.0	963	2.4
<i>B</i>	94	51.8	1.15	0.65	8.6	1.25	0.727	6.0	1122	1.8
<i>B'</i>	90	52.5	1.25	0.65	14.8	1.25	0.415	6.0	877	2.4
<i>B'</i>	92	51.6	1.25	0.65	10.3	1.25	0.618	6.0	1025	2.2
<i>C</i>	90	55.0	1.20	0.70	8.8	1.25	0.65	6.2	1015	7.3
<i>C</i>	92	55.1	1.20	0.70	9.4	1.25	0.65	6.2	1041	5.1
<i>C</i>	94	55.6	1.20	0.70	9.1	1.25	0.62	6.2	1051	2.8
<i>C'</i>	90	54.9	1.20	0.70	8.4	1.25	0.65	6.2	1005	3.5
<i>C'</i>	92	55.0	1.20	0.70	9.0	1.25	0.65	6.2	1034	1.1
<i>D</i>	90	54.2	1.220	0.607	5.4	1.293	0.737	7.9	964	1.3
<i>D</i>	92	54.5	1.231	0.596	9.2	1.181	0.668	6.4	951	1.2
<i>D</i>	94	55.2	1.216	0.646	8.3	1.180	0.768	6.5	1071	0.6
<i>D'</i>	90	52.6	1.235	0.640	6.0	1.241	0.763	7.9	1005	1.8
<i>D'</i>	92	53.8	1.228	0.637	8.2	1.189	0.718	7.4	1013	0.5

Polarization Phenomena of Nucleons, Karlsruhe, 1965, edited by P. Huber and H. Schopper (W. Rosch and Co., Berne, Switzerland, 1966).

and compared to the data in Fig. 4. The data for ^{90}Zr and ^{92}Zr are fairly well fitted but those for ^{94}Zr are not.

Analyses of other proton data, especially at 11 MeV, have suggested that one of the best ways of improving the fits to scattering from a sequence of isotopes is to vary a' , the imaginary diffuseness.¹⁴ A similar trend had been observed in the analysis of proton scattering from ^{90}Zr at 18.8 MeV¹ and from $^{92,94}\text{Zr}$ at 19.4 MeV.² Allowing a' to vary, along with V and W_D , produced a substantial improvement in the fits to the present data also, especially for ^{94}Zr , as shown in Fig. 4. The resulting parameters are given as set B in Table IV. Although W_D and a' vary considerably amongst the three isotopes, the product $a'W_D$ is about 6.3 MeV in each case. This is very similar to the values for $a'W_D$ found at 19 MeV when $r_0' = 1.25$ F was used.

In passing, it should be remarked that although potentials A and B used "independent" spin-orbit coupling ($r_s = 1.12$ F, $a_s = 0.47$ F), this has little effect on the results. Indeed, simply setting $r_s = r_0$, $a_s = a$ with these potentials only affects the cross sections for $\theta \gtrsim 150^\circ$, although, of course, the predicted polarizations differ even for small θ .

The analyses^{1,2} at 19 MeV had implied that the Zr isotopes required a smaller value for r_0 and a larger value for a ; the optimum fits yielded $r_0 \approx 1.10$ to 1.15 F and $a \approx 0.75$ to 0.77 F. A compromise average geometry had been chosen for these data with $r_0 = 1.20$ F and $a = 0.70$ F, together with $r_0' = 1.25$ F and $a' = 0.65$ F. Hence it was of interest to test this geometry on the 12.7-MeV data also. The optimum values of V and W_D (with V_s fixed at the value used at 19 MeV) are included

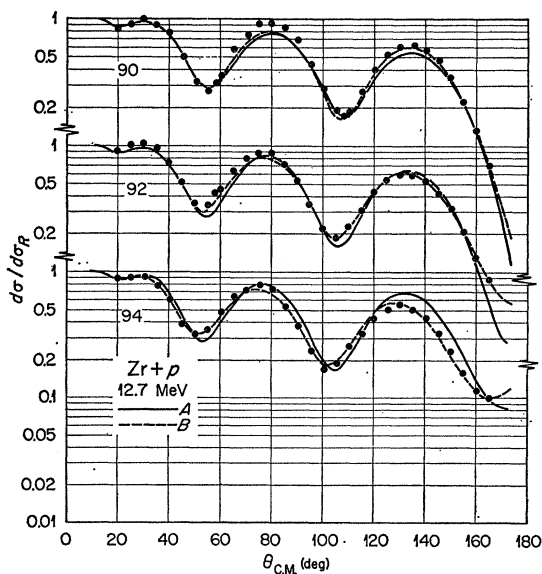


FIG. 4. Comparison of the measured elastic cross sections (in ratio to the Rutherford cross sections) with the curves calculated using the optical-model parameter sets A and B of Table IV.

¹⁴ C. M. Perey and F. G. Perey (private communication).

in Table IV as set C and the predictions compared to the data in Fig. 5. Only for ^{94}Zr does this geometry give a markedly better fit than that of set A, and this is presumably due to the larger value of a' which is used.

Since one might anticipate that the additional parameters most likely to vary with energy are r_0' and a' , these were also optimized, starting from set C. As a result the total χ^2 was nearly halved and both parameters increased in value for each isotope, their average values being close to $r_0' = 1.3$ and $a' = 0.7$. The total χ^2 , however, was still considerably larger than was obtained with set B with one less free parameter.

Finally, all the parameters were varied to minimize χ^2 , leading to set D of Table IV. The corresponding predictions are compared to the data in Fig. 5. The total χ^2 is now roughly half that obtained with set B, with

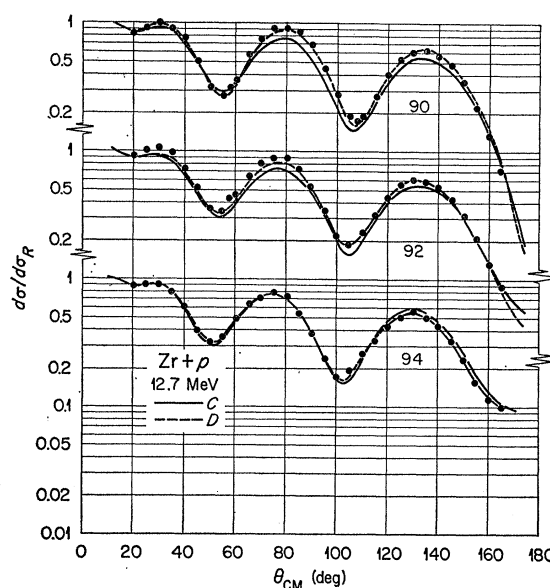


FIG. 5. Comparison of the measured elastic cross sections (in ratio to the Rutherford cross sections) with the curves calculated using the optical-model parameter sets C and D of Table IV.

the optimum r_0 and a values consistently smaller. However, r_0 is larger and a is smaller than the optimum values^{1,2} at 19 MeV, and this is in accord with the trends which seem to emerge when analyses of proton scattering at different energies are compared. The optimum parameters for the imaginary potential fluctuate considerably, but fall roughly within the same range as those found at 19 MeV.

There were some indications that the optical-model fits to the data would be improved if the cross sections for $^{90,92}\text{Zr}$ were reduced by about 10%. For example, the cross sections predicted for the second peak near $\theta = 80^\circ$ remain lower than measured even with the optimum set D. In addition, the ^{92}Zr cross sections for the peak near $\theta = 30^\circ$ remain consistently about 10% higher than the predictions for all potentials. For these reasons,

parameter sets A' , B' , C' , and D' were obtained by searching with these cross sections multiplied by 0.90. A substantial reduction in χ^2 results for the A -type potential but the advantage disappears when a' is allowed to vary, yielding set B' . The renormalization produces an even more dramatic reduction in χ^2 for the C -type potential, but again this advantage is lost when all the parameters are optimized to obtain set D' . The dependence of the parameters upon the normalization is quite similar to that reported in a recent study of these effects.¹⁵ A variation of about 10% in the cross-section magnitudes is possible with the present data. However, only for ^{92}Zr is the quality of fit improved by renormalization when all the parameters are optimized. Otherwise, a reduction in χ^2 is obtained only when the geometrical parameters are constrained to be the same for all three isotopes. One may judge (see Figs. 4 and 5) that the cross sections quoted¹⁰ for ^{92}Zr are too large by as much as 10%, but for the purpose of this paper we assume that renormalization is not required. Nonetheless, the optical-model results are quoted here for completeness and as examples of the kind of changes that a small error in normalization would induce.

An interesting feature of the present results is the lack of any clear evidence for a simple symmetry dependence of the real potential on $(N-Z)/A$. For example, the prescription given by Perey¹² for V when the real geometry of sets A and B is used yields $V = 53.1$ (90), 53.6 (92), and 54.2 (94), whereas sets A and B have values of V which are a little smaller and almost the same for each isotope. The well depths for the optimum sets D do show an increase with $(N-Z)/A$ of the order anticipated, but this is associated with some variations in the radius r_0 and diffuseness a . However, one should not conclude necessarily that here is evidence against the symmetry dependence. The changes expected are quite small and could easily be obscured by any irregularities in the data which might bias the optical-model search.¹⁵

IV. INELASTIC SCATTERING

A. General Remarks

The spectra of states excited in the present measurements are in good agreement with previously reported levels in these nuclei. Weak transitions observed here to states at 4.12 and 5.29 MeV in ^{90}Zr , 2.18 and 3.18 MeV in ^{92}Zr , and 3.39 MeV in ^{94}Zr were not seen in earlier work. In addition, the levels previously given at 2.85 MeV in ^{92}Zr and 2.34 MeV in ^{94}Zr are probably close doublets.

The ground and first 2^+ and 4^+ states of ^{92}Zr and ^{94}Zr are believed to be well described as states of a ^{90}Zr core plus two neutrons or two neutron holes, respectively, in the $2d_{5/2}$ orbit.⁵ Consequently, one would expect both the excitation energies and the cross

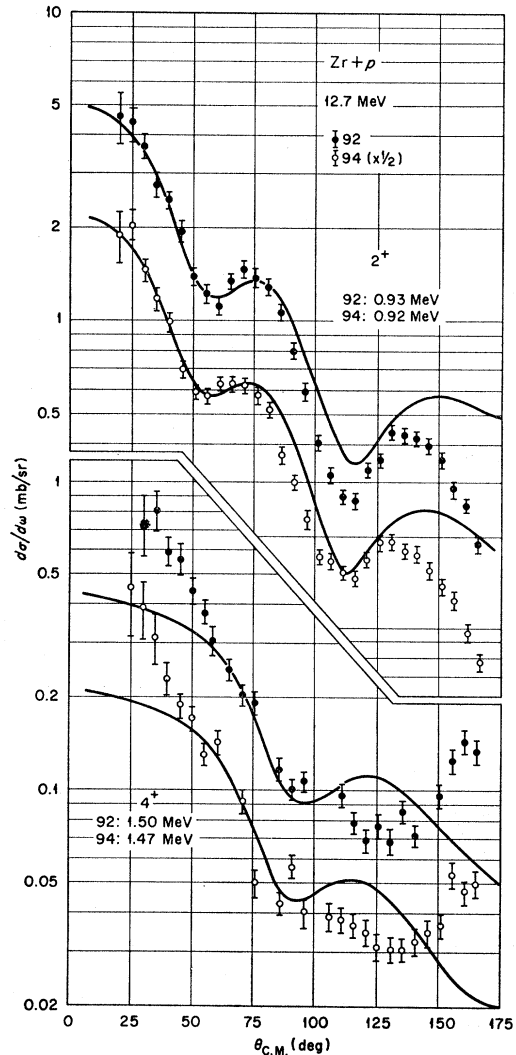


Fig. 6. Proton scattering from the lowest 2^+ and 4^+ levels in ^{92}Zr and ^{94}Zr , showing the similarities. Note the scaling factors. The curves are theoretical calculations for $L=2$ and 4 using the collective model as described in Sec. IV.

sections for these 2^+ and 4^+ states in ^{92}Zr to be almost the same as those for ^{94}Zr . Indeed the excitation energies of these states are nearly equal in the two isotopes, and Fig. 6 shows their differential cross sections are very similar also. In addition, there should be a series of excited states corresponding to excitations of the ^{90}Zr core coupled to these extra $d_{5/2}$ neutrons, with similar energies and differential cross sections in the two isotopes. One such pair, for an excitation of 2.49 MeV in ^{92}Zr and of 2.61 MeV in ^{94}Zr , is shown in Fig. 7. Neither is well fitted by the distorted-wave curves to be discussed below, but the similarities between the two sets of measurements suggest that these two excitations have the same spin and parity and have similar structure.

Two examples of marked similarities between the

¹⁵ J. K. Dickens, Phys. Rev. **143**, 758 (1966).

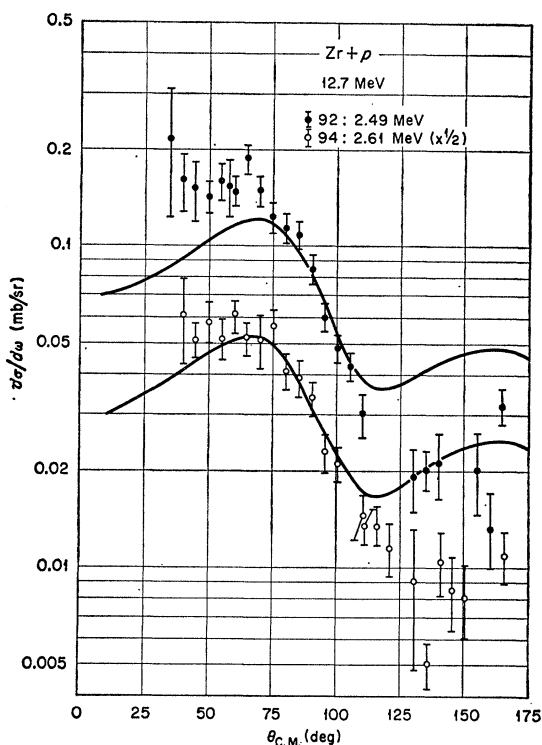


FIG. 7. Proton scattering from the 2.49-MeV level in ^{92}Zr compared with that for the 2.62-MeV level in ^{94}Zr . Note the scaling factors. The similarity of the angular distributions suggests that the spins and parities are the same. The theoretical curves are for $L=5$ and use the collective model interaction.

results from all three isotopes are provided by the excitations of the lowest 0^+ and 3^- states. The 3^- excitation is strong in each case and these states are commonly interpreted as octupole vibrations. Figure 8 compares the differential cross sections for these three transitions; it will be noted that the ^{92}Zr and ^{94}Zr results are closely similar, with the ^{90}Zr distribution showing small differences. It is possible that the latter are due to the excitation of the 4^- level in ^{90}Zr which is almost degenerate with the 3^- level, although previous experience suggests that non-normal parity levels such as this are very weakly excited. It should be noted that the energy of this 3^- level is steadily decreasing as A increases, so that small variations in its excitation might be expected.

The other interesting triad is provided by the 0^+ states at 1.75 (90), 1.37 (92), and 1.30 MeV (94). The measured differential cross sections are shown in Fig. 9. The 0^+ assignment for the 1.30-MeV level in ^{94}Zr had been surmised previously,² and the similarity of the present results to those for the 1.37-MeV 0^+ level in ^{92}Zr make this identification very convincing. Again, Fig. 9 indicates some differences between ^{90}Zr and the other two isotopes. All three states are expected to be due to the proton configuration which is orthogonal to the mixture present in the ^{90}Zr core ground state,⁵

$$|0^+\rangle = a|(2p_{1/2})^2, 0^+\rangle + b|(1g_{9/2})^2, 0^+\rangle. \quad (3)$$

However, there is independent evidence¹⁶ from $(d,^3\text{He})$ pickup reactions that the configuration mixture is modified by the presence of the extra neutrons, so that we should expect some variation with A in the excitation of these states.

B. Distorted-Wave Analysis

The theoretical predictions for the inelastic scattering were computed in the distorted-wave approximation.¹⁷ This treats the interaction V between the target nucleus and projectile proton to first order only, so that multiple excitation^{18,19} is neglected (except insofar as its effects on the elastic scattering are included in an average way by the use of optical potentials which fit the observed elastic scattering²⁰). For the interaction V we make use of the so-called collective model which identifies V with the nonspherical parts of the optical potential U when this is deformed in shape. For a given multipole

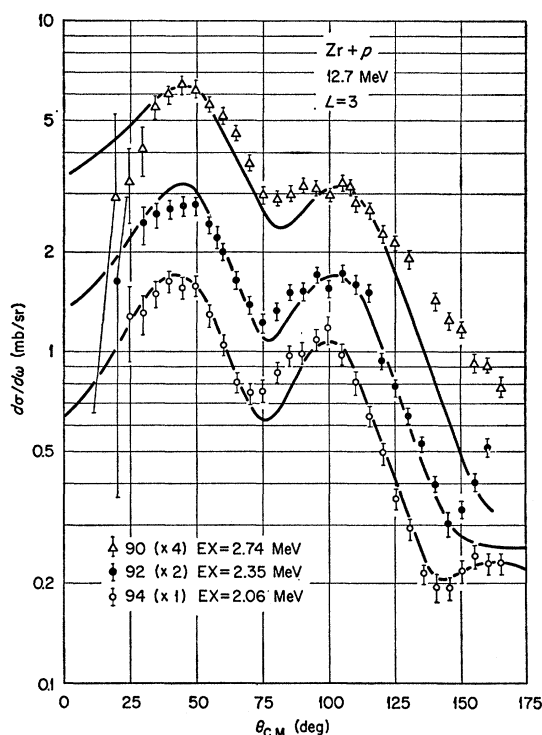


FIG. 8. Proton scattering from the lowest 3^- levels in $^{90,92,94}\text{Zr}$. Note the scaling factors; the absolute magnitudes are very similar. The curves are theoretical calculations for $L=3$ using the collective model.

¹⁶ B. M. Freedom, University of Tennessee Ph.D. thesis, 1967 (unpublished); and (to be published).

¹⁷ See, for example, G. R. Satchler, Nucl. Phys. **55**, 1 (1964) and other references cited there.

¹⁸ T. Tamura, Rev. Mod. Phys. **37**, 679 (1965).

¹⁹ W. G. Love, G. R. Satchler, and T. Tamura, Phys. Letters **22**, 325 (1966).

²⁰ F. G. Perey and G. R. Satchler, Phys. Letters **5**, 3 (1963).

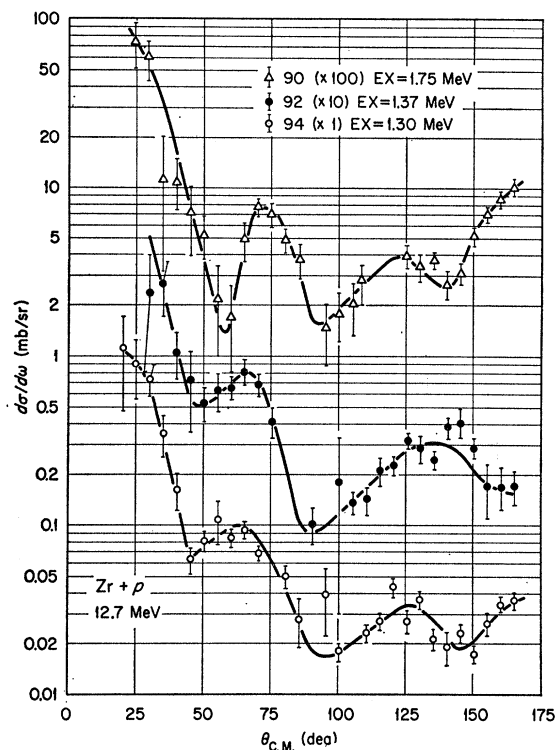


FIG. 9. Proton scattering from the lowest excited 0^+ levels in $^{90,92,94}\text{Zr}$. The curves have been included to guide the eye and are not the results of shrewd theoretical insight.

L , this gives a reduced nuclear matrix element²¹

$$\langle f || V || i \rangle \propto \beta_L (d/dr) U(r). \quad (4)$$

Since the parameters of $U(r)$ are determined by fitting to the elastic scattering data, only the strength or deformation parameter β_L is adjustable. In the distorted-wave approximation, the angular distribution is determined by the shape of $U(r)$ and the multipolarity L , while the magnitude of the cross section is proportional to β_L^2 . Hence we may identify the angular-momentum transfer L , and assign a measure of the transition strength through the β_L value.

This procedure is well established as a technique for extracting L values and parametrizing transition strengths, and has had considerable success in correlating the results of different measurements of these quantities.²² It is worth stressing, however, that its success in fitting angular distributions does not necessarily imply that the states being excited are described well by the collective model. Other models of the interaction (such as the microscopic shell model to be discussed below) will differ only in the radial shape; and if this should be peaked at the nuclear surface it will give the same results

²¹ R. H. Bassel, G. R. Satchler, R. M. Drisko, and E. Rost, *Phys. Rev.* **128**, 2693 (1962).

²² See, for example, J. S. Blair and F. G. Perey in *Nuclear Spin-Parity Assignments*, edited by N. B. Gove and R. L. Robinson (Academic Press Inc., New York, 1966).

as the collective model. Further, the gross features of the angular distribution are determined by the L transfer, and are much less sensitive to the radial shape of the interaction. In this way we may justify the use of the collective-model interaction as a spectroscopic tool which is independent of adjustable parameters. Nonetheless, we shall see that we sometimes encounter ambiguities when it is applied to the present data.

The collective model itself implies that the total angular-momentum transfer is the same as the multipolarity, $J=L$, and the parity change is $(-)^L$. This would only allow (to first order) the excitation of normal parity states with $I=L$, $\pi=(-)^L$ if the target has zero spin and even parity. If we admit the possibility of a spin-dependent interaction V which can induce spin-flip during the excitation, we can have $J=L\pm 1$ also and non-normal parity states may be excited. However, there is no evidence of these states being excited appreciably and it is a reasonable assumption that the states observed have normal parity. (See Ref. 1 for a further discussion of this.)

Although in principle the optical-potential parameters are predetermined by the elastic scattering data, we have seen that there are ambiguities and uncertainties in that analysis also. To ensure that the inelastic scattering predictions were not strongly affected by these uncertainties, calculations were performed using all of the parameter sets given in Table IV for all of the 2^+ and 3^- levels and for the 4^+ and 5^- levels in ^{90}Zr . The largest variations among the calculated angular distributions were for large values of scattering angle, but none of the calculated angular distributions for a given reaction was sufficiently different from the average of the calculated distributions for that reaction to warrant special comment. For the remainder of this paper, the "best-fit" set- D potentials were used.

The strong transitions exciting the 3^- levels shown in Fig. 8 are most likely to be collective. Indeed, the curves predicted by the collective-model interaction which are included in Fig. 8 are in good agreement with the data. Both the real and imaginary parts of the optical potential were deformed to obtain these curves. The fits are not as good as those obtained at 19 MeV for ^{90}Zr , but are of comparable quality for the other two isotopes. The deformation parameters β_3 corresponding to these curves are given in Tables I–III, and also agree well with those extracted from the 19-MeV data.^{1,2} The values obtained, $\beta_3 \approx 0.17$ – 0.18 , are similar to those obtained for the lowest-octupole excitation in other nuclei, and are about four or five times larger than those for a conventional "single-particle" transition.²³

C. Excitations of ^{90}Zr

The differential cross sections for exciting the various states in ^{90}Zr are shown in Figs. 10–13. The curves

²³ G. R. Satchler, R. H. Bassel, and R. M. Drisko, *Phys. Letters* **5**, 256 (1963).

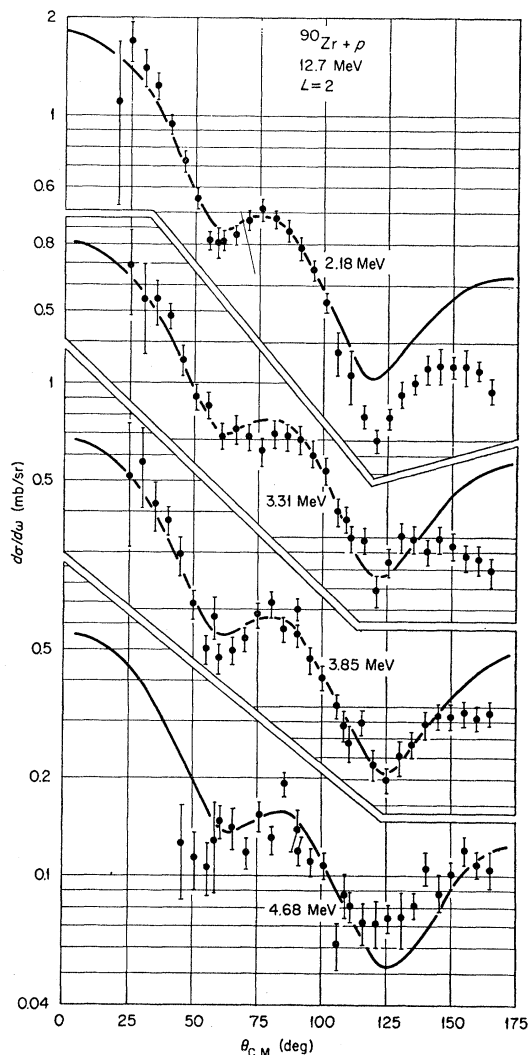


FIG. 10. Measured cross sections for some 2^+ states in ^{90}Zr . The curves are theoretical calculations for $L=2$ using the collective model; the deformation parameters are given in Table I.

shown are predictions obtained with the collective model interaction and the set- D potential parameters. As will be discussed, several of these curves are for illustrative purposes only and are not intended to imply definite L assignments.

The levels at 2.18 MeV (Fig. 10), 3.09 MeV and 3.45 MeV (Fig. 12) are believed to be due primarily to the 2^+ , 4^+ , and 6^+ states, respectively, of the $(1g_{9/2})^2$ proton configuration. (The 8^+ member at 3.6 MeV was too weakly excited to be seen clearly in the present experiment.) The $L=2, 4,$ and 5 theoretical curves are in good agreement with these data and the corresponding β_L values are given in Table I. The value of β_2 is close to that obtained at 18.8 MeV and that for β_4 is somewhat larger, while β_6 has less than half the value found at the higher energy. This last may not be

significant in view of the large uncertainties in the 3.45-MeV data.

Another state in ^{90}Zr believed to have a simple structure is the 5^- state at 2.32 MeV (Fig. 11), which is assigned to the $(2p_{1/2}, 1g_{9/2})$ proton configuration.⁵ The data for the excitation of this level are in good agreement with the $L=5$ theoretical curve, although the value of β_5 needed is larger than that found with 19-MeV protons by about 20%.

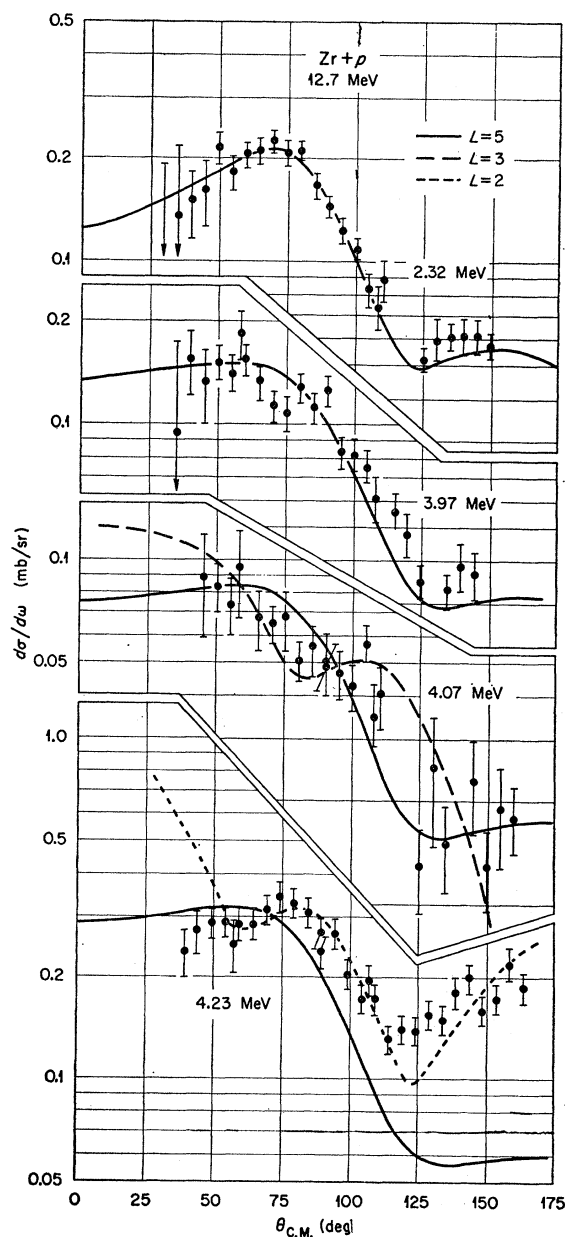


FIG. 11. Measured cross sections for one certain and some possible 5^- states in ^{90}Zr . The theoretical curves were obtained using the collective model and the deformation parameters given in Table I.

The measurements for the transitions to the levels at 3.31 and 3.85 MeV (Fig. 10) are in close agreement both with the predictions for $L=2$ and with the measurements for the 2^+ level at 2.18 MeV. The assignment 2^+ to these states seems secure. The group at 4.68 MeV (Fig. 10) also appears to be a 2^+ excitation. The present data are not very complete, but the angular distribution

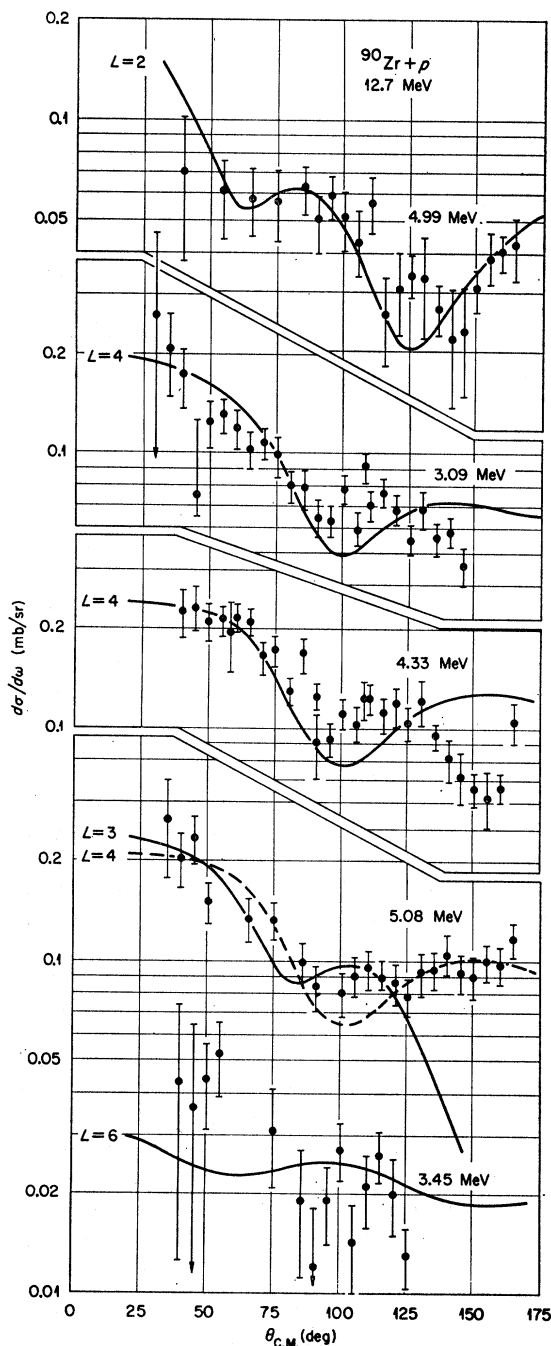


FIG. 12. Measured cross sections for some other states in ^{90}Zr . The theoretical curves were obtained using the collective model and the deformation parameters given in Table I.

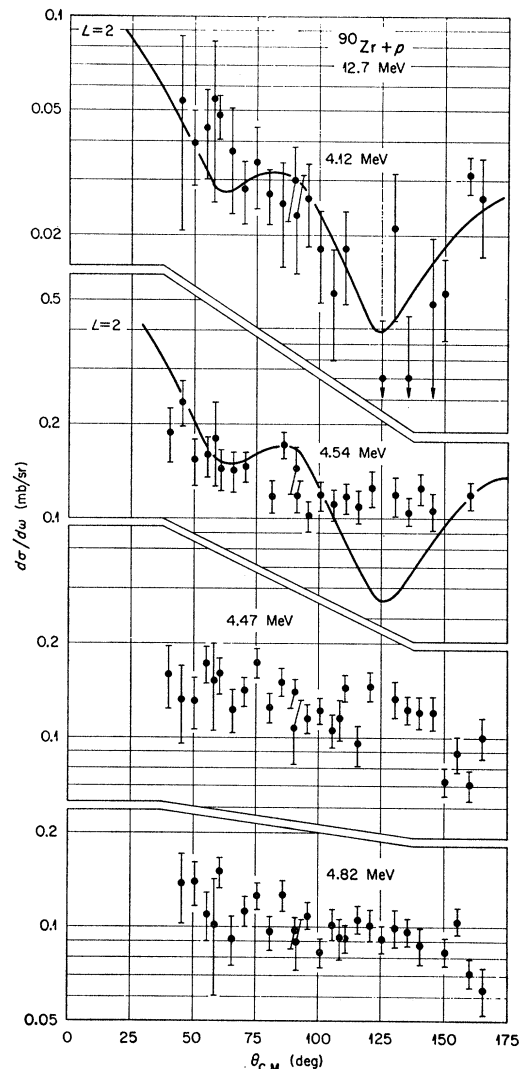


FIG. 13. Measured cross sections for some other states in ^{90}Zr . The theoretical curves were obtained using the collective model and the deformation parameters given in Table I.

measured at 19 MeV is in agreement with this choice. Another candidate is the level at 4.99 MeV, although this identification must be treated with caution since the transition is weak and the experimental errors are large. Even-parity levels are reported²⁴ at 4.65 and 4.98 MeV from the $^{89}\text{Y}(^3\text{He}, d)$ reaction; since $\ell_p=1$ is observed, they must be 0^+ , 1^+ , or 2^+ .

The level at 3.97 MeV yields an angular distribution which is close to that predicted for $L=5$. The same is true for excitation by protons of 19 MeV, and this level has also been identified as 5^- by the inelastic scattering of α particles.²⁵ The latter experiment excites the 3.97-MeV level with a relative strength of 38% of that

²⁴ G. S. Vourvopoulos and J. D. Fox, Phys. Letters (to be published).

²⁵ E. J. Martens and A. M. Bernstein, Phys. Letters **24B**, 669 (1967).

for the 5^- at 2.32 MeV, whereas the present data indicate the same value of β_5 for both transitions. The cross sections obtained with 19-MeV protons, however, have a ratio in agreement with the α measurements.

The same inelastic α scattering experiment²⁵ suggests the 4.33-MeV level has spin parity of 4^+ and both the present data (Fig. 12) and those taken with 19-MeV protons are consistent with $L=4$ transitions.

The identification of the remaining transitions in ^{90}Zr which were observed is more difficult. The differential cross sections measured for the weak 4.07-MeV group (Fig. 11) are compatible with either $L=3$ or 5. The results with 19-MeV protons look more like $L=3$, and it might be surprising to find another 5^- level only 100 keV from that at 3.97 MeV.

The very weak state at 4.12 MeV could be fed by an $L=2$ transition (Fig. 13). It does not appear to have been seen previously in either inelastic scattering or stripping reactions. The next state at 4.23 MeV is puzzling. Its excitation by 14.5- or 18.8-MeV protons yields angular distributions which are compatible with $L=5$ transitions. The 18.8-MeV data could also be interpreted as $L=6$. Figure 11 shows that the 12.7-MeV angular distribution is similar to that for $L=2$ for $\theta \gtrsim 55^\circ$. Comparison with either the $L=5$ curve or the other $L=5$ transitions at 2.32 and 3.97 MeV makes this assignment unlikely. Further, the $^{89}\text{Y}(^3\text{He},d)$ reaction²⁴ excites a state at 4.23 MeV with $\ell_p=1$, whose spin parity therefore must be 0^+ , 1^+ , or 2^+ . Of course, it is possible there is a close doublet of levels at this excitation energy in ^{90}Zr .

The 4.54-MeV excitation (Fig. 13) has a structureless angular distribution. The $L=2$ curve is shown only because this state may be the same as that seen at 4.56 MeV in the $^{89}\text{Y}(^3\text{He},d)$ reaction.²⁴ Since the transferred proton has $\ell_p=1$, the state has even parity and could have spin 2. The measurements with 19-MeV protons did not separate this level from that at 4.47 MeV. In the present experiment, the excitation of the latter (Fig. 13) shows even less structure in its angular distribution and no attempt to assign an L value could be made. The same is true for the transition to the 4.82-MeV level (Fig. 13). These may also correspond to levels (at 4.50 and 4.78 MeV) fed by the $^{89}\text{Y}(^3\text{He},d)$ reaction²⁴ through $\ell_p=1$ proton capture which, therefore, could be 0^+ , 1^+ , or 2^+ .

The remaining excitation, of 5.08 MeV, for which an angular distribution is available, may be due to two levels reported²⁴ at 5.08 and 5.10 MeV which are excited by $\ell_p=2$ proton capture. Hence they have odd parity and spins between 0 and 3. α scattering shows²⁵ an excitation at 5.12 MeV which is identified as octupole with a transition strength of 6.4% of that to the 3^- at 2.75 MeV. For illustrative purposes, both $L=3$ and 4 curves are shown in Fig. 12 with the present data for this 5.08-MeV excitation. It does not seem that a meaningful identification can be made.

D. Excitations of ^{92}Zr

The cross sections for the 2^+ state at 0.39 MeV and the 4^+ state at 1.50 MeV are shown in Fig. 6 together with the theoretical curves for $L=2$ and 4. The $L=2$ curve is in reasonably good agreement with the measurements except that it is somewhat too high for $\theta \gtrsim 85^\circ$. The $L=4$ curve is significantly different from the data both at forward angles and for $\theta \gtrsim 110^\circ$. Very similar discrepancies were observed for both groups in the experiment² with 19-MeV protons. It seems likely that the simple shell-model structure of these states is influencing the inelastic scattering in some way that is not reproduced by the collective-model interaction that we are using. If this is so, data on their excitation could be important for testing more microscopic descriptions of the scattering such as that to be discussed below.

The results for the 2.49-MeV level have already been mentioned and are compared in Fig. 7 to the very similar results for the 2.61-MeV level in ^{94}Zr . The $L=5$ curves in Fig. 7 indicate that these could be 5^- states due to the proton excitation corresponding to the 2.32-MeV 5^- state in ^{90}Zr . The measurements² on the excitation of these levels by 19-MeV protons support this assignment, while the similarity of the β_5 values required to that for the 2.32-MeV level in ^{90}Zr agree with the proton-excitation interpretation.

The remaining angular distributions measured for ^{92}Zr are shown in Fig. 14. The 1.85-MeV level has²⁶ spin parity 2^+ and the $L=2$ curve shown is in reasonable agreement with the data. It is tempting to surmise that this is a proton excitation corresponding to the $(g_{9/2})^2$, 2^+ state at 2.18 MeV in ^{90}Zr . It is fed by the $^{91}\text{Zr}(d,p)$ reaction²⁷ with $\ell_n=2$ capture, but with an intensity three to four times smaller than that to the first 2^+ state at 0.93 MeV, so that there is an admixture of some 25 to 30% of neutron $(d_{5/2})^2$, 2^+ excitation also.

The $^{91}\text{Zr}(d,p)$ reaction²⁷ excites the 2.07-MeV state by $\ell_n=0$ capture, indicating that it is at least partly a $(d_{5/2}, s_{1/2})$ neutron excitation, and has even parity with spin 2 or 3. Studies of the ^{92}Y decay²⁶ suggest 2^+ . However, Fig. 14 shows that the measured angular distribution for this transition does not agree with the $L=2$ curve; indeed it differs markedly from the measured 2^+ distributions for the 1.85- and 0.93-MeV states. The measured distribution is well fitted by the theoretical $L=4$ curve, but $L=4$ is not allowed for a 2^+ excitation. The distributions measured with 14.7-MeV protons⁷ and with 19-MeV protons² appear to differ from their respective $L=2$ predictions in a similar way, but they do not resemble their respective $L=4$ predictions at these energies. It seems likely that here is another example where it is important to take account of the

²⁶ M. E. Bunker, B. J. Dropesky, J. D. Knight, and J. W. Starmer, Phys. Rev. **127**, 844 (1962).

²⁷ H. J. Marten, M. B. Sampson, and R. L. Preston, Phys. Rev. **125**, 942 (1962); B. L. Cohen and O. V. Chubensky, *ibid.* **131**, 2184 (1963); J. K. Dickens and E. Eichler, Nucl. Phys. **A101**, 408 (1967).

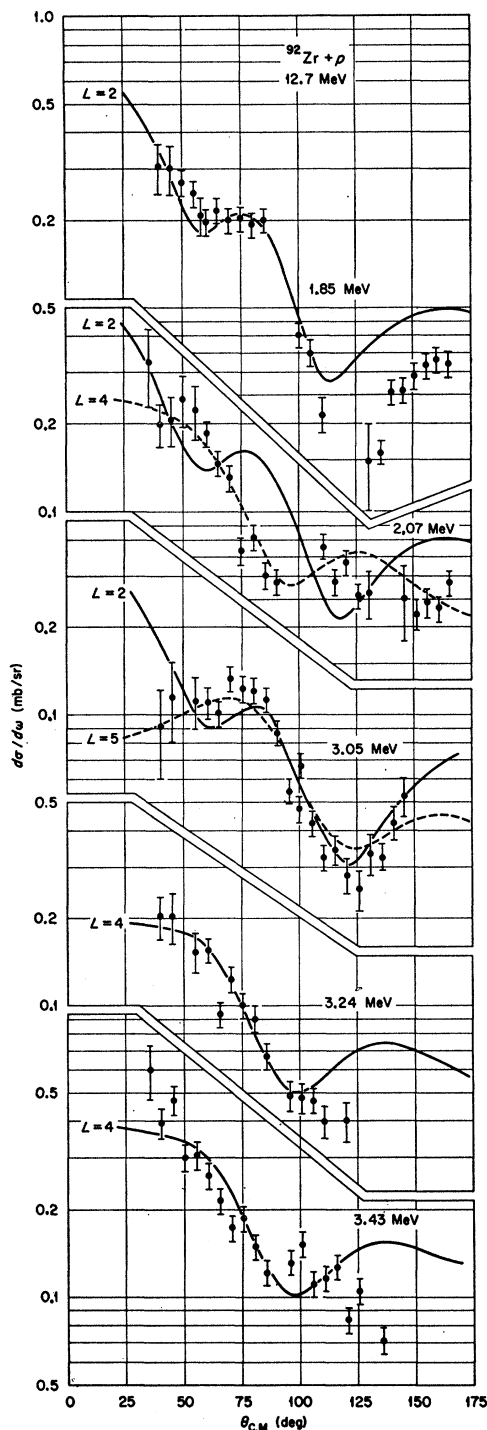


FIG. 14. Measured cross sections for states excited in ^{92}Zr . The theoretical curves were obtained using the collective model and the deformation parameters given in Table II.

nuclear structure in more detail rather than just the collective-model interaction.

The interpretation of the present data for the 3.05-MeV level would also be ambiguous without the aid of

other evidence. Figure 14 shows they are consistent with $L=2$ or 5, with some preference for the latter. However, a state variously reported at 3.08 and 3.06 MeV is also formed by $\ell_n=0$ neutron capture, indicating 2^+ or 3^+ . This favors $L=2$ for the proton scattering if it is the same state. The measurements with 19-MeV protons are also in nice agreement with $L=2$. The results of these experiments suggest this is a state containing most of the remaining ($d_{5/2}, s_{1/2}$) neutron 2^+ excitation strength. It seems likely that the 2.93-MeV level, strongly excited by $\ell_n=0$ capture²⁷ but not seen by proton scattering, corresponds to the 3^+ state of this neutron configuration.

The interpretation of the proton groups corresponding to excitations of 3.24, 3.32, and 3.43 MeV is uncertain. Levels at 3.21 and 3.28 MeV are excited by the $^{91}\text{Zr}(d, p)$ reaction, with $\ell_n > 0$. The apparent absence of $\ell_n=0$ capture suggests 2^+ and 3^+ assignments are unlikely. The 3.24-MeV proton group may correspond to one of these levels. Its angular distribution (Fig. 14) is in good agreement with the theoretical predictions for $L=4$. Its strength is similar to that for the 3.09-MeV 4^+ state in ^{90}Zr , so that it could be due to the same ($g_{9/2}$)² proton configuration. The 3.32-MeV proton group presumably is exciting the same 3.32-MeV level seen in the (d, p) reaction. Its angular distribution, however, is very similar to that of the 3.24-MeV group (with a strength about $\frac{2}{3}$ as great), whereas the $\ell_n=0$ transition of the (d, p) reaction implies spin parity 2^+ or 3^+ . (However, the angular distribution for this excitation with 19-MeV protons² most closely resembles that for an $L=5$ transition.) The angular distribution (Fig. 14) of the protons exciting ^{92}Zr to 3.43 MeV also resembles that of the 3.24-MeV group, but in this case the width of the 3.43-MeV group suggests that more than one level may be contributing. The $L=4$ curve is included in Fig. 14 merely to facilitate comparison of the two distributions.

E. Excitations of ^{94}Zr

The data for the 2^+ , 0.92-MeV and 4^+ , 1.47-MeV states (Fig. 6) have been discussed already; they are very similar to those for the corresponding transitions in ^{92}Zr , and differ from the theoretical curves in the same way. The 2.61-MeV results were also discussed in the previous section, where it was suggested that this level and that at 2.49 MeV in ^{92}Zr correspond to the 5^- level at 2.32 MeV in ^{90}Zr .

The remaining angular distributions measured are shown in Fig. 15. The state at 1.66 MeV is clearly excited by an $L=2$ transition, just as with 19-MeV protons.² The distribution is similar to that for the 1.85-MeV state in ^{92}Zr , and we may speculate that these are mainly the 2^+ state of the ($g_{9/2}$)² proton configuration corresponding to the 2.18-MeV state in ^{90}Zr . Their transition strengths are also comparable.

An excitation of 2.34 MeV has been previously

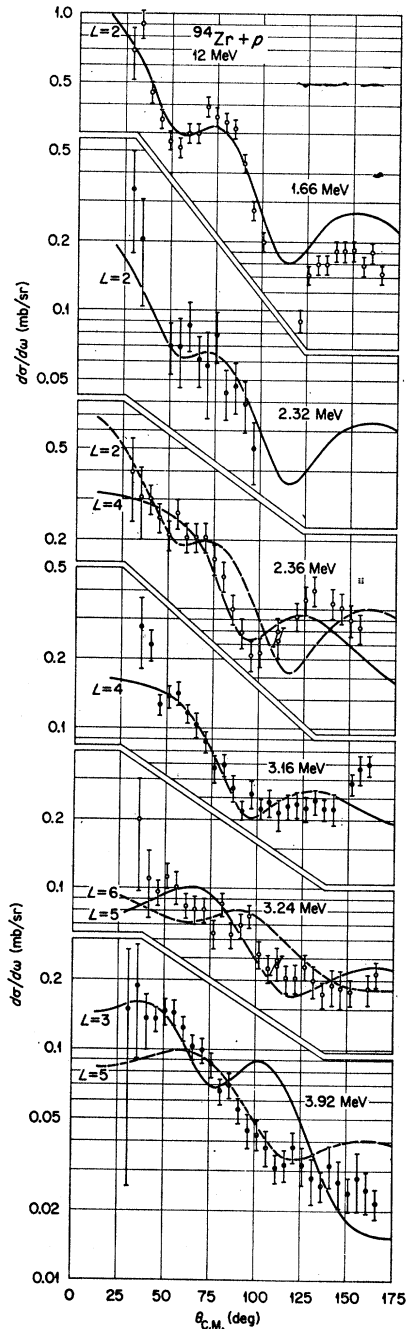


FIG. 15. Measured cross sections for states excited in ^{94}Zr . The theoretical curves were obtained using the collective model and the deformation parameters given in Table III.

reported,^{2,28} but the present experiment sees two groups at 2.32 and 2.36 MeV. The 2.32-MeV angular distribution is compatible with $L=2$, while that for 2.36 MeV more closely resembles $L=4$. Since it would be surprising to find two 2^+ states so close in energy we tentatively

²⁸ R. K. Jolly, E. K. Lin, and B. L. Cohen, Phys. Rev. **128**, 2292 (1962).

suggest 2^+ for the 2.32-MeV level and 4^+ for the 2.36-MeV level.

The 3.16-MeV angular distribution is satisfactorily described as due to an $L=4$ transition (Fig. 15). Its strength is similar to that for the 3.24-MeV level in ^{92}Zr and the 3.09-MeV 4^+ level in ^{90}Zr , so all three may be due primarily to the same excitation of the $(g_{9/2})^2$ proton configuration.

Values of $L=4, 5$, or 6 are possible for the 3.24-MeV excitation (Fig. 15), although the lack of similarity to the 3.16-MeV transition may argue against $L=4$. The choice $L=6$ implies a surprisingly large value for β_6 , so we tend to favor $L=5$ for this transition. Similar confusion exists over the interpretation of the 3.92-MeV angular distribution. Excitation of this level by deuterons²⁸ has been taken to indicate negative parity, but Fig. 15 shows that neither $L=3$ or 5 gives a satisfactory account of the data. Indeed, $L=2$ or 4 yield as good results.

V. APPLICATION OF THE SHELL MODEL

A microscopic description^{3,4} of the inelastic scattering uses the more detailed wave functions of shell-model theory for the target nucleus in order to evaluate the matrix elements on the left side of Eq. (4). For the interaction V a single scattering approximation is made,

$$V = \sum_i v_{ip}, \quad (5)$$

where the sum runs over the active nucleons in the target and p refers to the projectile. The simplest model for the effective two-body interaction v_{ip} is a local, real, and central potential of the form often used in shell-model calculations for bound-state properties, namely

$$v_{ip} = -(V_0 + V_1 \sigma_i \cdot \sigma_p) g(r_{ip}), \quad (6)$$

with

$$V_s = V_{s\alpha} + V_{s\beta} \tau_i \cdot \tau_p. \quad (7)$$

The various angular-momentum transfers L come from the usual multipole expansion^{3,29} of the function $g(r_{ip})$, while the $S=1$ term allows an additional transfer of unity through spin flip. It has been argued¹ that the contributions from this spin-spin interaction are much smaller than from the spin-independent $S=0$ term, and we shall not discuss them further here.³⁰ The isospin dependence enters upon comparing the excitation of the valence protons in ^{90}Zr (for which we should use $V_{s\alpha} + V_{s\beta}$) with the excitation of the valence neutrons in $^{92,94}\text{Zr}$ (for which we should use $V_{s\alpha} - V_{s\beta}$).

²⁹ D. M. Brink and G. R. Satchler, *Angular Momentum* (Oxford University Press, New York, 1962).

³⁰ An unambiguous determination of the strength V_1 of the spin-spin interaction requires the measurement of the excitation of a state known to have nonnormal parity and whose wave function is understood with some confidence. $J=L\pm 1$ only for these transitions and hence only V_1 can contribute to first order. Appropriate examples in the Zr isotopes would be the 3^+ state of the $(d_{5/2}, s_{1/2})$ neutron configuration and the 4^- state of the $(g_{9/2} p_{1/2})$ proton configuration.

Previous studies³ indicated that a Yukawa form for $g(r_{ip})$ with a range close to 1 F gave a satisfactory interpretation of proton scattering from a variety of nuclei. This work considered only the direct interaction between the projectile and the valence nucleons, for example, the last two protons in ^{90}Zr . It has since been realized that virtual excitations of the core may also play an important role. These will also contribute to electromagnetic transitions between the same initial and final states, and give rise to the need to use "effective charges" when computing transition rates with shell-model wave functions. This fact was used in a recent attempt⁶ to estimate the importance of this core polarization for inelastic scattering. A simple collective model was used for the core, so for each L value the virtual core excitation is a surface vibration of the same multipolarity. The parameters needed are determined by the electric-transition rate or $B(EL)$, where this is available. Unfortunately, with one exception, this number is available only for $L=2$. This makes the range of the v_{ip} interaction more difficult to

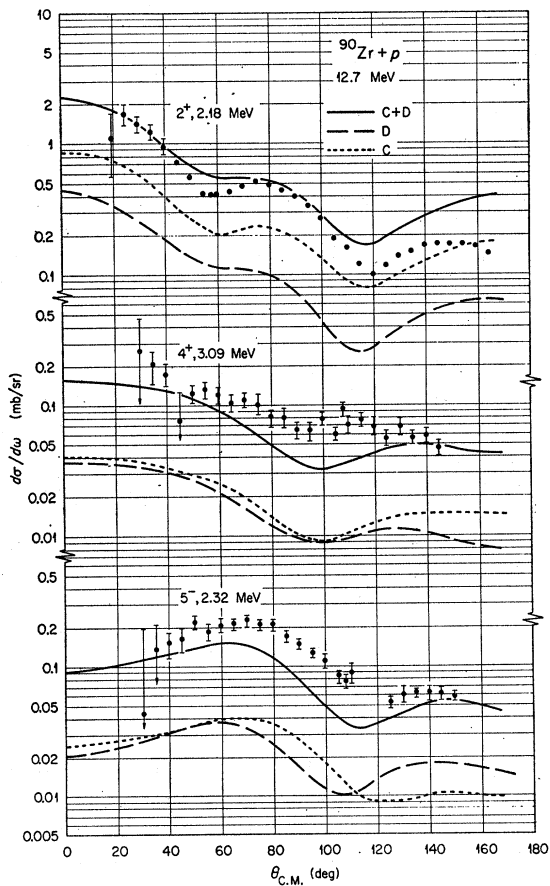


FIG. 16. Comparison of the predictions of the microscopic model with the measured cross sections for some states in ^{90}Zr . The dashed curves D are the cross sections for direct coupling alone, the dotted curves C are for core excitation alone, while the full curves C+D include both contributions and their interference.

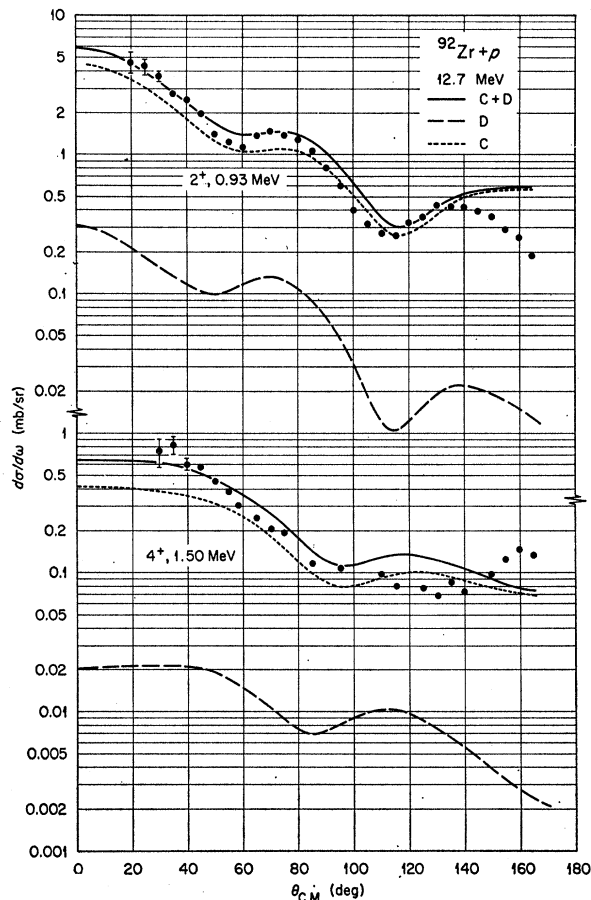


FIG. 17. Comparison of the predictions of the microscopic model with the measured cross sections for some states in ^{92}Zr . The dashed curves D are the cross sections for direct coupling alone, the dotted curves C are for core excitation alone, while the full curves C+D include both contributions and their interference.

determine because it mainly affects the relative strengths of different multipoles. The exception is the decay of the 5^- level at 2.32 MeV in ^{90}Zr , for which a value of $B(E5)$ is available. The exploratory calculations made so far⁶ show that the Yukawa form with a range of 1 F still appears to be satisfactory, although the strength required is only about one-half that needed without core polarization. The values $V_{0\alpha} \approx 80$ MeV, $V_{0\beta} \approx 20$ MeV give a reasonable account of the data.

Calculations were made for the present data with the parameter values all the same as previously described in Refs. 3 and 6, except that the optical potentials used were the sets D of Table IV appropriate for the energy of 12.7 MeV. The results are compared in Figs. 16 and 17 to the data for the excitation of the $(g_{9/2})^2$, 2^+ and 4^+ states and the $(g_{9/2}p_{1/2})$ state of ^{90}Zr , and the $(d_{5/2})^2$, 2^+ and 4^+ states of ^{92}Zr . The theoretical curves are for direct coupling strengths $V_{0\alpha} = 80$ MeV, $V_{0\beta} = 20$ MeV. Since the $E4$ transition strengths are not known, it was assumed that the 2^4 -pole core coupling was one-half the strength of the quadrupole coupling. This assumption

led to reasonable agreement⁶ with the 19-MeV data for ^{90}Zr , and corresponds to an effective charge of $1.7e$ for the valence protons in ^{90}Zr and $0.9e$ for the valence neutrons in ^{90}Zr for these $E4$ transitions.

Also shown in Figs. 16 and 17 are the cross sections predicted using the core polarization alone (C) and the direct coupling alone (D). (There is, of course, interference between the two amplitudes when both are included.) The relative importance of the core polarization here is very similar to that found for 19-MeV protons, as was shown in Fig. 1 of Ref. 6, for example. Namely, the core term alone contributes about half the quadrupole cross section for ^{90}Zr and nearly all of it for ^{92}Zr . (The direct coupling strength for the former, $V_{0\alpha} + V_{0\beta} = 100$ MeV, is nearly twice that for the latter, $V_{0\alpha} - V_{0\beta} = 60$ MeV.) The core and direct coupling amplitudes are roughly equal for the $L=4$ and 5 transitions in ^{90}Zr , but the core term dominates again for $L=4$ in ^{92}Zr .

The inclusion of Coulomb excitation would improve the agreement with experiment for the quadrupole excitations. The measured cross sections for the 4^+ and 5^- states in ^{90}Zr are both larger than predicted. A similar, but not so large, discrepancy was noted for $L=5$ at 19 MeV. There is a large uncertainty in the value of the core-coupling strength for this multipole, partly from an uncertainty in the $B(E5)$ itself, and partly from uncertainty in the value of $\langle r^5 \rangle$ which is required. Thus this cross section could easily be increased. There is no independent evidence for the $L=4$ core coupling strength, although the value assumed here gave rough agreement with the 19-MeV data for this transition. The fact that both $L=4$ and 5 multipole cross sections are low here, whereas the quadrupole remains in agreement with the measurements, might be taken to suggest that the effective interaction has a shorter range at 12.7 MeV. For this reason, the calculations were repeated using a Yukawa interaction of range 0.7 F. The predicted quadrupole cross sections are found to be almost identical with those shown in Fig. 16; a strength $V_{0\alpha} + V_{0\beta} = 220$ MeV is used. However, with this strength the new $L=4$ and 5 cross sections also agree with the old ones to within about 4%, so there is no improvement.

Figure 17 shows that reasonable agreement with the measurements for ^{92}Zr is obtained without further adjustment of parameters.³¹ Calculations were also made for ^{92}Zr with an interaction with a shorter range of 0.7 F, but again an increased strength of $V_{0\alpha} - V_{0\beta} \approx 100$ MeV yields essentially the same cross sections as those for the 1 F range shown in Fig. 17. The direct contributions are so small for ^{92}Zr that it is difficult to extract an unambiguous value for their strength. The

³¹ It was stated in Ref. 6 that the cross section for exciting the 4^+ state by 19.4-MeV protons required an effective charge about 0.8 times that for the quadrupole transition. This was due to an arithmetical error. In fact, $e_{\text{eff}}(L=4)/e_{\text{eff}}(L=2) \approx 0.4$ gives cross sections in fair agreement with the measurements.

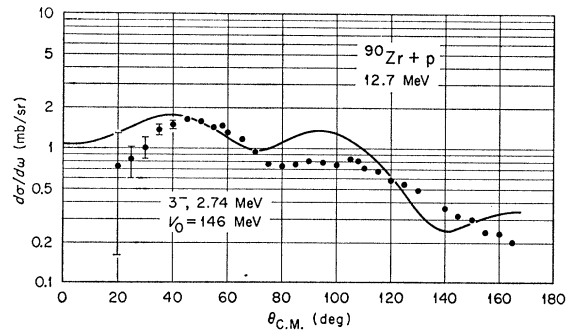


FIG. 18. Comparison with the data of the theoretical cross sections for the 3^- level in ^{90}Zr . Microscopic hole-particle wave functions were used for the 3^- state together with a direct coupling of range 1 F and strength 146 MeV.

figure of 60 MeV used here with the 1 F range was chosen, as in Ref. 6, to be consistent with the strength $V_{0\beta} \approx 20$ MeV found necessary to give the observed (p,n) transition rate between analog states.

If very complete nuclear wave functions were available, it would be unnecessary to introduce the concepts of effective charges or core polarization. A step in this direction is taken when one uses, for example, mixtures of hole-particle configurations to describe the 3^- octupole excitation in ^{90}Zr . Calculations of the TDA type³² have been performed for the odd-parity levels of ^{90}Zr by Kunz,³³ and his hole-particle wave functions for the 3^- state at 2.75 MeV were used to calculate the (p,p') cross sections shown in Fig. 18. Eleven hole-particle configurations were included, but excitations from the $1f_{7/2}$ shell (included by Kunz) were neglected. Again the effective interaction was represented by a Yukawa form with a range of 1 F. Corresponding calculations³ for 18.8-MeV protons using the same form factor required a strength $V_{0\alpha} \approx 150$ MeV in order to reproduce the peak cross section observed at that energy. The curve drawn in Fig. 18 was normalized with this same strength. Again the peak cross-section magnitude is reproduced correctly, but the angular distribution is in much poorer agreement with the data than that predicted by the simple collective model (compare with Fig. 8). A similar, but not so marked, discrepancy was noted for the higher-energy results.³ The explanation of this discrepancy (which is similar to those observed in calculations^{3,4} for transitions of the same type in other nuclei) is not known at present, but it is likely to be due to the use of an oversimplified form for the effective interaction.

The strength required for this octupole transition is larger by almost a factor of 2 than the $V_{0\alpha} \approx 80$ MeV which we have found for the other transitions when core polarization was included. Some of the excess is due to

³² A. M. Lane, *Nuclear Theory* (W. A. Benjamin, Inc., New York, 1964); G. Brown, *Unified Theory of Nuclear Models* (Interscience Publishers, Inc., New York, 1964).

³³ P. D. Kunz, *Bull. Am. Phys. Soc.* **9**, 179 (1964); and (private communication).

the omission of the $1f_{7/2}$ excitations from the form factor, and the remainder may be a measure of the inadequacy of the restriction to one hole-one particle excitations. Certainly the inclusion of ground-state correlations (as included in the random-phase approximation,³² for example) often produce enhancements of transition probabilities by factors of order 2.

VI. 0^+ EXCITATIONS

Monopole $L=0$ transitions are unusual in that their angular distributions are particularly sensitive to the interaction form-factor shape. To illustrate this, calculations were made with a number of simple form factors. By analogy with the collective model for other multipoles, the reduced nuclear-matrix element was parametrized as

$$\langle 0^+, \text{Ex.} || V || 0^+, \text{g.s.} \rangle = \beta_0 g(r) / (4\pi)^{1/2}.$$

The three choices made for $g(r)$ were

$$g(r) = U(r), \quad R dU/dr, \quad R^2 d^2U/dr^2,$$

where $U(r)$ is the real part of the optical-model potential. These are representative of interactions which are uniform through the nuclear volume, peaked on the surface, or peaking and changing sign at the surface, respectively. The predicted differential cross sections are shown in Fig. 19. The volume interaction gives an angular distribution with very little structure, whereas the second derivative form leads to marked oscillations.

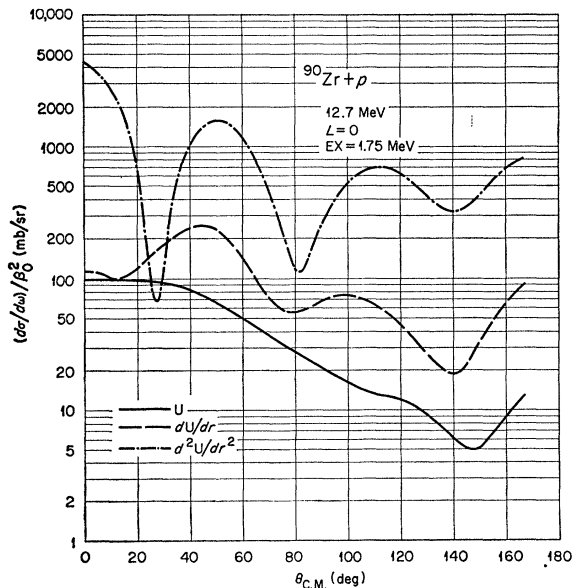


FIG. 19. Theoretical cross sections for monopole excitations in ^{90}Zr using the three different interaction form-factor shapes described in the text.

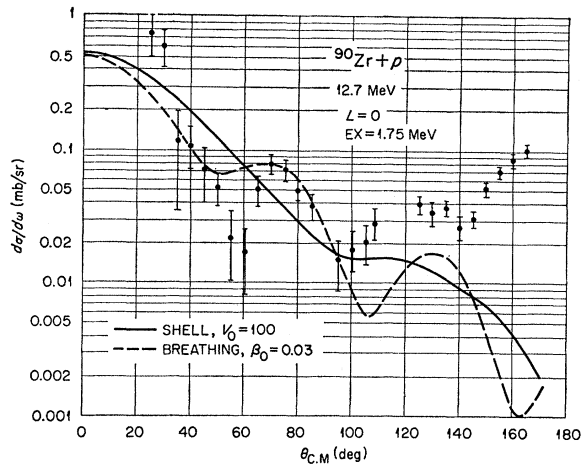


FIG. 20 Cross sections for excitation of the lowest 0^+ level in ^{90}Zr . The solid curve was calculated using shell-model wave functions and a Yukawa interaction of range 1 F. The dashed curve is for a breathing mode collective oscillation.

These features are characteristic of monopole transitions in other targets and at other energies also.

The measured angular distributions for excitation of the lowest 0^+ states in the Zr isotopes (Fig. 9) do show an appreciable structure which is not like any of the curves in Fig. 19. However, this is not surprising. The 1.75-MeV 0^+ states in ^{90}Zr is believed to be due to the configuration mixture which is complementary to that, Eq. (3), for the ground state, and one may assume the 0^+ state seen in the other two isotopes has an analogous structure. Hence one might expect the microscopic model described in the previous section to be appropriate. We have no reason to expect strong collective monopole oscillations of the core, so that the core polarization effects should be small. Figure 20 shows the results of calculations using the Yukawa direct interaction with a range of 1 F, and the wave-function parameters $a=0.8$, $b=0.6$. [The predicted cross section is directly proportional to $(ab)^2$.] The theoretical cross sections with $V_{0\alpha} + V_{0\beta} = 100$ MeV have the same order of magnitude as those measured, but the angular distribution does not have the observed oscillations. The lack of structure in the angular distribution is due to the shape of the form factor.³ This is very large in the nuclear interior and hence yields an angular distribution similar to that shown in Fig. 19 for the volume interaction. In fact, Fig. 19, suggests that one way to reproduce the observed structure is to have the interaction enhanced in some way near the nuclear surface. (It is not sufficient to dampen the interior contributions alone, because this makes the cross section unacceptably small.)

The measurements with 18.8-MeV protons only gave³ upper limits on the cross sections for this 0^+ level. At

that time, the core polarization effects were not considered and it was believed the direct coupling strength was $V_0 \approx 200$ MeV. This predicted much too large cross sections for the 0^+ state.³⁴

Other, collective, models are possible for 0^+ excitations in nuclei.³⁵ While it does not seem very reasonable to apply them to the present case, the predictions for a simple breathing mode of oscillation are included in Fig. 20. The angular distribution has the same qualitative features as the data. In this model, dilation of the radius of the optical potential U gives an interaction term proportional to dU/dr , while the requirement of volume conservation introduces a volume term proportional to U and of opposite sign.³⁶ The sum of these two terms changes sign just inside the nuclear surface, and it seems to be this feature which produces the maxima and minima in the angular distribution. It is interesting to note that a density-dependent effective interaction³⁶ would produce a form factor of this type with the shell-model wave functions of Eq. (3), provided it was much weaker inside nuclear matter than in the surface region. Of course, any new model of this type for the interaction would have to be applied to the other multipole transitions also, in order to check for consistency. In any case, it seems that data on these monopole excitations will be a valuable testing ground for later theoretical developments.

³⁴ In addition, a factor (ab) was omitted from the theoretical cross sections given by Johnson *et al.* in Ref. 3. The curves shown in Fig. 7 of that reference should be reduced in magnitude by this factor (ab)=0.48.

³⁵ G. R. Satchler, Nucl. Phys. A100, 481 (1967).

³⁶ A. Migdal, in *Many-Body Description of Nuclear Structure and Reactions*, edited by C. Bloch (Academic Press Inc., New York, 1967); T. H. R. Skyrme, Nucl. Phys. 9, 615 (1959).

VII. SUMMARY

The differential cross sections for elastic scattering and for the excitation of numerous levels in $^{90,92}\text{Zr}$ have been measured. Optical-model potentials were obtained by fitting to the elastic data; it was found that the optimum parameter values differed somewhat from those found by analysis of 19-MeV scattering data.^{1,2} Distorted-wave calculations using these parameters and the usual "collective"-model interaction were then used where possible to assign multipolarities to the inelastic transitions and to deduce strength parameters β_L . These generally agreed with those found at other bombarding energies, but some ambiguous and puzzling cases were discussed.

A microscopic description of the inelastic scattering using shell-model wave functions was also investigated for a few transitions. The effects of core polarization were included and found to contribute a large fraction of the observed cross sections. A direct coupling to the valence nucleons of the same strength as that found at higher energies and for other nuclei gave reasonable agreement with the present data. On the other hand, there are serious discrepancies with the angular distributions for the excitation of the lowest 0^+ and 3^- levels, which imply that the form of effective interaction being used is oversimplified.

ACKNOWLEDGMENTS

We are indebted to G. Chiosi and R. J. Silva for assistance with the data accumulation and to G. F. Wells for excellent accelerator operation during the experiment. R. M. Drisko kindly made available the distorted-wave code JULIE and optical-model search code HUNTER. W. G. Love assisted with the core-polarization calculations.